Acta Mechanica Solida Sinica, Vol. 22, No. 5, October, 2009 ISSN 0894-9166
Published by AMSS Press, Wuhan, China

HYBRID FEM WITH FUNDAMENTAL SOLUTIONS AS TRIAL FUNCTIONS FOR HEAT CONDUCTION SIMULATION

Hui Wang[1] **Qing-Hua Qin**[2⋆]
([1] *College of Civil Engineering and Architecture, Henan University of Technology, Zhengzhou* 450052*, China*)
([2] *Department of Engineering, Australian National University, Canberra, ACT* 0200*, Australia*)

Received 3 August 2009, revision received 12 September 2009

ABSTRACT A new type of hybrid finite element formulation with fundamental solutions as internal interpolation functions, named as HFS-FEM, is presented in this paper and used for solving two dimensional heat conduction problems in single and multi-layer materials. In the proposed approach, a new variational functional is firstly constructed for the proposed HFS-FE model and the related existence of extremum is presented. Then, the assumed internal potential field constructed by the linear combination of fundamental solutions at points outside the elemental domain under consideration is used as the internal interpolation function, which analytically satisfies the governing equation within each element. As a result, the domain integrals in the variational functional formulation can be converted into the boundary integrals which can significantly simplify the calculation of the element stiffness matrix. The independent frame field is also introduced to guarantee the inter-element continuity and the stationary condition of the new variational functional is used to obtain the final stiffness equations. The proposed method inherits the advantages of the hybrid Trefftz finite element method (HT-FEM) over the conventional finite element method (FEM) and boundary element method (BEM), and avoids the difficulty in selecting appropriate terms of T-complete functions used in HT-FEM, as the fundamental solutions contain usually one term only, rather than a series containing infinitely many terms. Further, the fundamental solutions of a problem are, in general, easier to derive than the T-complete functions of that problem. Finally, several examples are presented to assess the performance of the proposed method, and the obtained numerical results show good numerical accuracy and remarkable insensitivity to mesh distortion.

KEY WORDS hybrid FEM, fundamental solution, variational functional, heat conduction

I. INTRODUCTION

During the past decades, research into the development of efficient finite elements has been mostly concentrated on the following three distinct types of FEM[1–6]. The first is the conventional FEM. It is based on a suitable polynomial interpolation which has already been used to analyze most engineering problems. With this method, the solution domain is divided into a number of small cells or elements, and material properties are defined at element level[1]. The second is the natural-mode FEM. In contrast, the natural FEM, initiated by Argyris et al.[2], presents a significant alternative to conventional FEM with ramifications on all aspects of structural analysis. It makes distinction between the constitutive and geometric parts of the element tangent stiffness, which could lead effortlessly to the non-linear

⋆ Corresponding author. E-mail: qinghua.qin@anu.edu.au

effects associated with large displacements. When applied to composite structures, the physically clear and comprehensible theory with complete quadrature elimination and avoidance of modal (shape) functions can show distinctly the mechanical behavior of isotropic and composite shell structures[2,3]. The final is the so-called hybrid Trefftz FEM (HT-FEM)[4,6]. Unlike in the conventional and natural FEM, the HT-FEM couples the advantages of FEM[1] and BEM[7]. In contrast to conventional FEM and BEM, HT-FEM is based on a hybrid method which includes the use of an independent auxiliary inter-element frame field defined on each element boundary and an independent internal field chosen so as to a prior satisfy the homogeneous governing differential equations by means of a suitable truncated T-complete function set of homogeneous solutions. Inter-element continuity is enforced by using a modified variational principle, which is used to construct the standard force-displacement relationship, that is, stiffness equation, and establish linkage of frame fileds and internal fields of the element. The property of nonsingular element boundary integral that appears in HT-FEM enables us to construct arbitrarily shaped element conveniently; however, the terms of truncated T-complete functions should be carefully selected in achieving desired results. Further, they are difficult to develop for some physical problems. To remove the drawback of HT-FEM, a novel hybrid finite formulation based on the fundamental solution, named as HFS-FEM, is firstly developed for solving two dimensional heat conduction problems in single and multilayer-materials. The proposed HFS-FEM can be viewed as the fourth type of FEM which is significantly different from the previous three types of FEM discussed above. In the analysis, a linear combination of the fundamental solution at different points is used to approximate the field variable within the element. The independent frame field defined along the element boundary and the newly developed variational functional are employed to guarantee the inter-element continuity, generate the final stiffness equation and establish linkage between the boundary frame field and internal field in the element. The proposed HFS-FEM inherits all advantages of HT-FEM and removes the difficulty in constructing and selecting T-functions, so it can reach more extensive applications than the HT-FEM. Moreover, it is necessary to point out that the developed approach is different from the BEM, although the same fundamental solution is employed. Using the reciprocal theorem, the BEM obtains the boundary integral equation, which usually encounters difficulty in dealing with singular or hyper-singular integrals in the BEM analysis, while the proposed method can remove this weakness. Additionally, the more flexible element material definition in the HFS-FEM is important for multi-material analysis, rather than the material definition in the entire domain in the BEM.

The paper begins with a simple description of heat conduction problems in §II. Then, a detailed derivation of the proposed HFS-FEM and the corresponding algorithm is described in §III to provide an initial insight on this new finite element model. Several numerical examples are presented in §IV to validate the proposed algorithm and some concluding remarks are presented in §V.

II. STATEMENT OF HEAT CONDUCTION PROBLEMS

Consider that we are seeking to find the solution of a well-posed heat conduction problem in a general plane domain Ω

$$\frac{\partial}{\partial X_1}\left(k\frac{\partial u(\boldsymbol{x})}{\partial X_1}\right)+\frac{\partial}{\partial X_2}\left(k\frac{\partial u(\boldsymbol{x})}{\partial X_2}\right)=0 \qquad \forall \boldsymbol{x}\in\Omega \tag{1}$$

with the following boundary conditions:

—Dirichlet boundary condition related to the unknown temperature field

$$u=\bar{u} \quad \text{on } \Gamma_u \tag{2}$$

—Neumann boundary condition for the boundary heat flux

$$q=-ku_{,i}n_i=\bar{q} \quad \text{on } \Gamma_q \tag{3}$$

where k stands for the thermal conductivity, u is the sought field variable and q represents the boundary heat flux. n_i is the ith component of the outward normal vector to the boundary $\Gamma=\Gamma_u\cup\Gamma_q$, and $\bar{u}$ and $\bar{q}$ are specified functions on the related boundaries, respectively. The space derivatives are indicated by a comma, i.e. $u_{,i}=\partial u/\partial X_i$, and the subscript index i takes values 1 and 2 in our analysis. Additionally, the repeated subscript indices stand for the summation convention.

For the sake of convenience, Eq.(3) is rewritten in the matrix form as

$$q = -k\boldsymbol{A}\left\{\begin{array}{c} u_{,1} \\ u_{,2} \end{array}\right\} = \bar{q} \tag{4}$$

with $\boldsymbol{A} = \left\{ n_1 \; n_2 \right\}$.

III. BASIC FORMULATION OF HFS FINITE ELEMENT APPROACH

In this section, the procedure for developing a hybrid finite element model with fundamental solutions as interior trial functions is described based on the boundary value problem (BVP) defined by Eqs.(1)-(3).

Similar to HT-FEM, The main idea of the proposed approach is to establish a hybrid finite element formulation whereby intra-element continuity is enforced on a nonconforming internal displacement field formed by a linear combination of fundamental solutions at points outside the element domain under consideration, while an auxiliary frame field is independently defined on the element boundary to enforce the field continuity across inter-element boundaries. But unlike in HT-FEM, the intra-element field, is constructed based on the fundamental solution, rather than T-functions. Consequently, a variational functional corresponding to the new trial function is required to derive the related stiffness matrix equation. With the problem domain divided into some sub-domains or elements denoted by Ω_e with the element boundary Γ_e, the additional continuity is usually required on the common boundary Γ_{Ief} between any two adjacent elements 'e' and 'f' (see Fig.1):

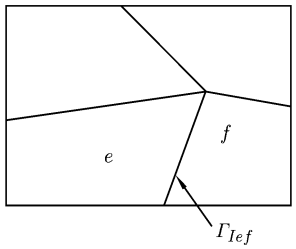

Fig. 1 Illustration of continuity between two adjacent elements 'e' and 'f'.

$$\left.\begin{array}{r} u_e = u_f \text{ (conformity)} \\ q_e + q_f = 0 \text{ (reciprocity)} \end{array}\right\} \text{ on } \Gamma_{Ief} = \Gamma_e \cap \Gamma_f \tag{5}$$

in the proposed hybrid FE approach.

3.1. Non-conforming Intra-element Field

Activated by the idea of the method of fundamental solutions (MFS)[8] to remove the singularity of fundamental solutions, for a particular element, say element e, which occupies sub-domain Ω_e, we first assume that the field variable defined in the element domain is extracted from a linear combination of fundamental solutions centered at different source points (see Fig.2), that is,

$$u_e(\boldsymbol{x}) = \sum_{j=1}^{n_s} N_e\left(\boldsymbol{x}, \boldsymbol{y}_j\right) c_{ej} = \boldsymbol{N}_e(\boldsymbol{x})\, \boldsymbol{c}_e \qquad \forall \boldsymbol{x} \in \Omega_e,\ \boldsymbol{y}_j \notin \Omega_e \tag{6}$$

where c_{ej} is undetermined coefficients and n_s is the number of virtual sources outside the element e. $N_e(\boldsymbol{x}, \boldsymbol{y}_j)$ is the fundamental solution to the 2D heat conduction and generally satisfies

$$k\nabla^2 N_e(\boldsymbol{x}, \boldsymbol{y}) + \delta(\boldsymbol{x}, \boldsymbol{y}) = 0 \qquad \forall \boldsymbol{x}, \boldsymbol{y} \in \mathbb{R}^2 \tag{7}$$

which gives

$$N_e(\boldsymbol{x}, \boldsymbol{y}) = -\frac{1}{2\pi k} \ln r(\boldsymbol{x}, \boldsymbol{y}) \tag{8}$$

where $\mathbb{R}^2$ refers to the infinite plane space and $r(\boldsymbol{x}, \boldsymbol{y})$ be the Euclidian distance of $\boldsymbol{x}$ and $\boldsymbol{y}$.

Evidently, Eq.(6) analytically satisfies Eq.(1) due to the solution property of $N_e(\boldsymbol{x}, \boldsymbol{y}_j)$.

In practice, the generation of virtual sources is usually done by means of the following formulation employed in the MFS[9, 10]:

$$\boldsymbol{y} = \boldsymbol{x}_b + \gamma(\boldsymbol{x}_b - \boldsymbol{x}_c) \tag{9}$$

where γ is a dimensionless coefficient, $\boldsymbol{x}_b$ is the elementary boundary point and $\boldsymbol{x}_c$ the geometrical centroid of the element. For a particular element shown in Fig.2, we can use the nodes of the element to generate related source points for simplicity.

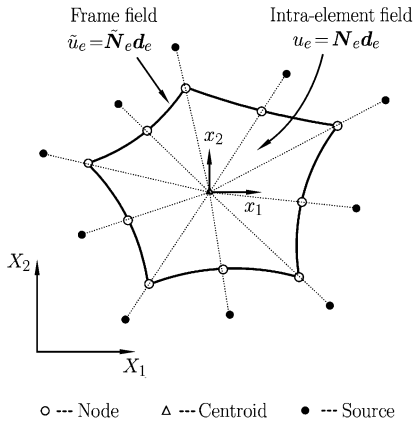

Fig. 2. Intra-element field, frame field in a particular element in HFS-FEM, and the generation of source points for a particular element.

The corresponding outward normal derivative of u_e on Γ_e is

$$q_e = -k\frac{\partial u_e}{\partial n} = \boldsymbol{Q}_e \boldsymbol{c}_e \tag{10}$$

where

$$\boldsymbol{Q}_e = -k\frac{\partial \boldsymbol{N}_e}{\partial n} = -k\boldsymbol{A}\boldsymbol{T}_e \tag{11}$$

with

$$\boldsymbol{T}_e = \begin{bmatrix} \dfrac{\partial \boldsymbol{N}_e}{\partial x_1} \\ \dfrac{\partial \boldsymbol{N}_e}{\partial x_2} \end{bmatrix} \tag{12}$$

3.2. Auxiliary Conforming Frame Field

In order to enforce the conformity on the field variable u, for instance, $u_e = u_f$ on $\Gamma_e \cap \Gamma_f$ of any two neighboring elements e and f, an auxiliary inter-element frame field $\tilde{u}$ is used and expressed in terms of the same degrees of freedom (DOF), $\boldsymbol{d}$, as used in the conventional finite elements. In this case, $\tilde{u}$ is confined to the whole element boundary, that is

$$\tilde{u}_e(\boldsymbol{x}) = \tilde{\boldsymbol{N}}_e(\boldsymbol{x})\,\boldsymbol{d}_e \tag{13}$$

which is independently assumed along the element boundary in terms of nodal DOF $\boldsymbol{d}_e$, where $\tilde{\boldsymbol{N}}_e$ represents the conventional finite element interpolating functions. For example, a simple interpolation of the frame field on the side with three nodes of a particular element (Fig.2) can be given in the form

$$\tilde{u} = \tilde{N}_1 u_1 + \tilde{N}_2 u_2 + \tilde{N}_3 u_3 \tag{14}$$

where $\tilde{N}_i$ $(i = 1, 2, 3)$ stands for shape functions in terms of the natural coordinate ξ defined in Fig.3.

3.3. Modified Variational Principle and Stiffness Equation

3.3.1. Modified functional

For the boundary value problem defined in Eqs.(1)-(3) and (5), since the stationary conditions of the traditional potential or complementary variational functional can't guarantee the satisfaction of the inter-element continuity condition required in the proposed HFS FE model, a modified potential functional is developed as follows

$$\Pi_m = \sum_e \Pi_{me} = \sum_e \left[\Pi_e + \int_{\Gamma_e} (\tilde{u} - u)\, q \mathrm{d}\Gamma\right] \tag{15}$$

where

$$\Pi_e = -\frac{1}{2}\int_{\Omega_e} k u_{,i} u_{,i} \mathrm{d}\Omega - \int_{\Gamma_{qe}} \bar{q}\tilde{u}\mathrm{d}\Gamma \tag{16}$$

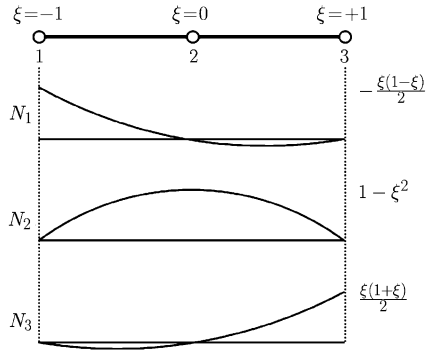

Fig. 3. Typical quadratic interpolation for the frame field.

in which the governing equation (1) is assumed to be satisfied, a *priori*, for deriving the HFS FE model. It should be mentioned that the functional (15) is different from that used in Ref.[5]. The boundary Γ_e of a particular element consists of the following parts

$$\Gamma_e = \Gamma_{ue} \cup \Gamma_{qe} \cup \Gamma_{Ie} \tag{17}$$

where Γ_{Ie} represents the inter-element boundary of the element 'e' shown in Fig.2.

• **Stationary condition of the proposed functional**

Next we will show that the stationary condition of the functional (15) leads to the governing equation (Euler equation), boundary conditions and continuity conditions. To this end, invoking Eqs.(16) and (15) gives the following functional for the problem domain

$$\Pi_{me} = -\frac{1}{2}\int_{\Omega_e} k u_{,i} u_{,i} \mathrm{d}\Omega - \int_{\Gamma_{qe}} \bar{q}\tilde{u}\mathrm{d}\Gamma + \int_{\Gamma_e} q\left(\tilde{u}-u\right)\mathrm{d}\Gamma \tag{18}$$

whose first-order variational yields

$$\delta\Pi_{me} = -\int_{\Omega_e} k u_{,i}\delta u_{,i}\mathrm{d}\Omega - \int_{\Gamma_{qe}} \bar{q}\delta\tilde{u}\mathrm{d}\Gamma + \int_{\Gamma_e}\left(\delta\tilde{u}-\delta u\right)q\mathrm{d}\Gamma + \int_{\Gamma_e}\left(\tilde{u}-u\right)\delta q\mathrm{d}\Gamma \tag{19}$$

Using the divergence theorem

$$\int_{\Omega} f_{,i}h_{,i}\mathrm{d}\Omega = \int_{\Gamma} h f_{,i} n_i \mathrm{d}\Gamma - \int_{\Omega} h\nabla^2 f \mathrm{d}\Omega \tag{20}$$

for any smooth functions f and h in the domain, we have

$$\delta\Pi_{me} = \int_{\Omega_e} k u_{,ii}\delta u\mathrm{d}\Omega - \int_{\Gamma_{qe}}\left(\bar{q}-q\right)\delta\tilde{u}\mathrm{d}\Gamma + \int_{\Gamma_{ue}} q\delta\tilde{u}\mathrm{d}\Gamma + \int_{\Gamma_{Ie}} q\delta\tilde{u}\mathrm{d}\Gamma + \int_{\Gamma_e}\left(\tilde{u}-u\right)\delta q\mathrm{d}\Gamma \tag{21}$$

For the displacement-based method, the potential conformity should be satisfied in advance, that is,

$$\begin{array}{ll} \delta\tilde{u} = 0 & \text{on } \Gamma_{ue} \quad (\tilde{u} = \bar{u}) \\ \delta\tilde{u}^e = \delta\tilde{u}^f & \text{on } \Gamma_{Ief} \quad (\tilde{u}^e = \tilde{u}^f) \end{array} \tag{22}$$

then, Eq.(21) can be rewritten as

$$\delta\Pi_{me} = \int_{\Omega_e} k u_{,ii}\delta u\mathrm{d}\Omega - \int_{\Gamma_{qe}}\left(\bar{q}-q\right)\delta\tilde{u}\mathrm{d}\Gamma + \int_{\Gamma_{Ie}} q\delta\tilde{u}\mathrm{d}\Gamma + \int_{\Gamma_e}\left(\tilde{u}-u\right)\delta q\mathrm{d}\Gamma \tag{23}$$

from which the Euler equation in the domain Ω_e and boundary conditions and Γ_q can be obtained

$$\begin{array}{ll} k u_{,ii} = 0 & \text{in } \Omega_e \\ q = \bar{q} & \text{on } \Gamma_{qe} \\ \tilde{u} = u & \text{on } \Gamma_e \end{array} \tag{24}$$

using the stationary condition $\delta\Pi_{me}=0$.

About the continuity requirement between two adjacent elements 'e' and 'f' given in Eq.(5), we can obtain it in the following way. When assembling elements 'e' and 'f', we have

$$\delta\Pi_{m(e+f)}=\int_{\Omega_{e+f}}ku_{,ii}\delta u\mathrm{d}\Omega-\int_{\Gamma_{qe}+\Gamma_{qf}}(\bar{q}-q)\,\delta\tilde{u}\mathrm{d}\Gamma+\int_{\Gamma_e}(\tilde{u}-u)\,\delta q\mathrm{d}\Gamma$$
$$+\int_{\Gamma_f}(\tilde{u}-u)\,\delta q\mathrm{d}\Gamma+\int_{\Gamma_{Ief}}\left(q^e+q^f\right)\delta\tilde{u}^{ef}\mathrm{d}\Gamma+... \tag{25}$$

from which the vanishing variation of $\Pi_{m(e+f)}$ leads to the reciprocity condition $q_e+q_f=0$ on the inter-element boundary Γ_{Ief}.

• **Theorem on the existence of extremum**

If the expression

$$\int_{\Gamma_q}\delta q\delta\tilde{u}\mathrm{d}s-\sum_e\left[\int_{\Gamma_{Ie}}\delta q_e\delta\tilde{u}_e\mathrm{d}s+\int_{\Gamma_e}\delta q_e\delta(\tilde{u}_e-u_e)\mathrm{d}s\right] \tag{26}$$

is uniformly positive (or negative) in the neighborhood of $\{u\}_0$, where the displacement $\{u\}_0$ has such a value that $\Pi_m(\{u\}_0)=(\Pi_m)_0$, and where $(\Pi_m)_0$ stands for the stationary value of Π_m, we have

$$\Pi_m\geq(\Pi_m)_0\quad[\text{ or }\Pi_m\leq(\Pi_m)_0] \tag{27}$$

in which the relation that $\{\tilde{u}\}_e=\{\tilde{u}\}_f$ is identical on $\Gamma_e\cap\Gamma_f$ has been used. This is due to the definition in Eq.(5) of §II.

PROOF: For the proof of the theorem on the existence of extremum, we may complete it by way of the so-called 'second variational approach'[11]. In doing this, performing variation of $\delta\Pi_m$ and using the constrained condition (26), we find

$$\delta^2\Pi_m=\int_{\Gamma_q}\delta q\delta\tilde{u}\mathrm{d}s-\sum_e\left[\int_{\Gamma_{Ie}}\delta q_e\delta\tilde{u}_e\mathrm{d}s+\int_{\Gamma_e}\delta q_e\delta(\tilde{u}_e-u_e)\mathrm{d}s\right]=\text{expression (18)} \tag{28}$$

Therefore the theorem has been proved from the sufficient condition of the existence of a local extreme of a functional[11]. This completes the proof.

3.3.2. Stiffness equation

Having independently defined the intra-element field and frame field in a particular element (see Fig.2), the next step is to generate the element stiffness equation through a variational approach.

Following the approach described in Ref.[5], the variational functional Π_e corresponding to a particular element e of the present problem can be written as

$$\Pi_{me}=-\frac{1}{2}\int_{\Omega_e}ku_{,i}u_{,i}\mathrm{d}\Omega-\int_{\Gamma_{qe}}\bar{q}\tilde{u}\mathrm{d}\Gamma+\int_{\Gamma_e}q\,(\tilde{u}-u)\,\mathrm{d}\Gamma \tag{29}$$

Applying the divergence theorem (20) again to the above functional, we have the final functional for the HFS FE model

$$\begin{aligned}\Pi_{me}&=\frac{1}{2}\left(\int_{\Gamma_e}qu\mathrm{d}\Gamma+\int_{\Omega_e}uk\nabla^2u\mathrm{d}\Omega\right)-\int_{\Gamma_{qe}}\bar{q}\tilde{u}\mathrm{d}\Gamma+\int_{\Gamma_e}q\,(\tilde{u}-u)\,\mathrm{d}\Gamma\\&=-\frac{1}{2}\int_{\Gamma_e}qu\mathrm{d}\Gamma-\int_{\Gamma_{qe}}\bar{q}\tilde{u}\mathrm{d}\Gamma+\int_{\Gamma_e}q\tilde{u}\mathrm{d}\Gamma\end{aligned} \tag{30}$$

Then, substituting Eqs.(6), (10) and (13) into the functional (30) finally produces

$$\Pi_{me}=-\frac{1}{2}\boldsymbol{c}_e^{\mathrm{T}}\boldsymbol{H}_e\boldsymbol{c}_e-\boldsymbol{d}_e^{\mathrm{T}}\boldsymbol{g}_e+\boldsymbol{c}_e^{\mathrm{T}}\boldsymbol{G}_e\boldsymbol{d}_e \tag{31}$$

in which

$$\boldsymbol{H}_e = \int_{\Gamma_e} \boldsymbol{Q}_e^{\mathrm{T}} \boldsymbol{N}_e \mathrm{d}\Gamma = \int_{\Gamma_e} \boldsymbol{N}_e^{\mathrm{T}} \boldsymbol{Q}_e \mathrm{d}\Gamma, \quad \boldsymbol{G}_e = \int_{\Gamma_e} \boldsymbol{Q}_e^{\mathrm{T}} \tilde{\boldsymbol{N}}_e \mathrm{d}\Gamma, \quad \boldsymbol{g}_e = \int_{\Gamma_{qe}} \tilde{\boldsymbol{N}}_e^{\mathrm{T}} \bar{q} \mathrm{d}\Gamma$$

The symmetry of $\boldsymbol{H}_e$ is obvious from the scale definition (31) of variational functional Π_{me}.

To enforce inter-element continuity on the common element boundary, the unknown vector $\boldsymbol{c}_e$ should be expressed in terms of nodal DOF $\boldsymbol{d}_e$. The minimization of the functional Π_{me} with respect to $\boldsymbol{c}_e$ and $\boldsymbol{d}_e$, respectively, yields

$$\frac{\partial \Pi_{me}}{\partial \boldsymbol{c}_e^{\mathrm{T}}} = -\boldsymbol{H}_e \boldsymbol{c}_e + \boldsymbol{G}_e \boldsymbol{d}_e = \boldsymbol{0}, \quad \frac{\partial \Pi_{me}}{\partial \boldsymbol{d}_e^{\mathrm{T}}} = \boldsymbol{G}_e^{\mathrm{T}} \boldsymbol{c}_e - \boldsymbol{g}_e = \boldsymbol{0} \tag{32}$$

from which the optional relationship between $\boldsymbol{c}_e$ and $\boldsymbol{d}_e$, and the stiffness equation can be produced

$$\boldsymbol{c}_e = \boldsymbol{H}_e^{-1} \boldsymbol{G}_e \boldsymbol{d}_e \text{ and } \boldsymbol{K}_e \boldsymbol{d}_e = \boldsymbol{g}_e \tag{33}$$

where $\boldsymbol{K}_e = \boldsymbol{G}_e^{\mathrm{T}} \boldsymbol{H}_e^{-1} \boldsymbol{G}_e$ stands for the element stiffness matrix.

It is worthy pointing out that the evaluation of the right-handed vector $\boldsymbol{g}_e$ in Eq.(33) is the same as that in the conventional FEM, which is obviously convenient for the implementation of HFS-FEM into an existing FEM program.

3.4. Recovery of Rigid-body Motion

Considering the physical definition of the fundamental solution, it's necessary to recover the missing rigid-body motion modes from the above results.

Following the method presented in Ref.[5], the missing rigid-body motion can be recovered by writing the internal potential field of a particular element e as

$$u_e = \boldsymbol{N}_e \boldsymbol{c}_e + c_0 \tag{34}$$

where the undetermined rigid-body motion parameter c_0 can be calculated using the least square matching of u_e and $\tilde{u}_e$ at element nodes[5]

$$\sum_{i=1}^{n} \left(\boldsymbol{N}_e \boldsymbol{c}_e + c_0 - \tilde{u}_e \right)^2 \Big|_{\text{node } i} = \min \tag{35}$$

which finally gives

$$c_0 = \frac{1}{n} \sum_{i=1}^{n} \Delta u_{ei} \tag{36}$$

in which $\Delta u_{ei} = (\tilde{u}_e - \boldsymbol{N}_e \boldsymbol{c}_e)|_{\text{node } i}$ and n is the number of element nodes.

Once the nodal field is determined by solving the final stiffness equation, the coefficient vector $\boldsymbol{c}_e$ can be evaluated from Eq.(33), and then c_0 is evaluated from Eq.(36). Finally, the potential field u at any internal point in an element can be obtained by means of Eq.(6).

IV. NUMERICAL ASSESSMENTS

In this section, two numerical examples are considered to demonstrate the basic principle, numerical accuracy, and insensitivity to mesh distortion of the proposed method. From the discussion above, it is found that an arbitrarily shaped element can be constructed easily with the model. However, considering the requirement of accuracy and computational simplification, 8-node parabolic quadrilateral elements are employed in this work, because they are extremely versatile for boundary matching and most pre-processing algorithms developed for conventional FEM used here. In other words, we can utilize the current pre-process procedure of the conventional FEM to obtain the desired mesh division in the present analysis.

In order to compare the influence of the generation of source points outside the selected 8-node element, the configurations shown in Fig.4 are employed, in which, 4, 8, 12 and 16 source points are generated by means of nodal points or middle points on the element boundary respectively and Eq.(9) is used to evaluate their locations.

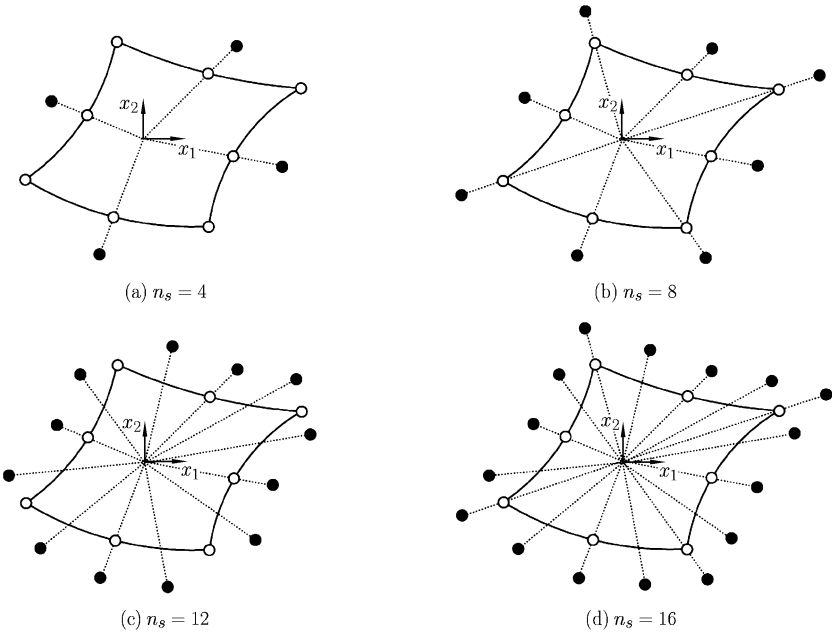

Fig. 4. Configurations of source points for a typical 8-node element.

In addition, in order to provide a more quantitative understanding of results, the average relative error (Arerr) on an arbitrary variable f is introduced as

$$\text{Arerr}\,(f) = \sqrt{\frac{\sum\limits_{i=1}^{N}\left(f_{\text{numerical}} - f_{\text{exact}}\right)_i^2}{\sum\limits_{i=1}^{N}\left(f_{\text{exact}}\right)_i^2}} \tag{37}$$

where N is the number of test points and $(f)_i$ is an arbitrary field function, such as the potential at point i.

Example 1. Heat conduction in a thick-walled cylinder

The first example is designed to verify the accuracy of the proposed formulations and investigate the effect of the location of source points, which are vital for almost all MFS-based methods. In this example, a thick cylinder with Dirichlet boundary conditions is considered. Due to the symmetric property of the problem, only one quarter of the entire domain is modeled and related boundary conditions are shown in Fig.5. The needed thermal conductivity is taken as 1 for simplicity. The analytical solution of this problem

$$u = a + b\ln r \tag{38}$$

where

$$a = \frac{u_i \ln(r_0) - u_0 \ln(r_i)}{\ln(r_0/r_i)}, \quad b = \frac{u_0 - u_i}{\ln(r_0/r_i)}$$

is used for comparison.

In the calculation, $r_i = 5$, $r_0 = 20$, $u_i = 10$, $u_0 = 0$ are assumed and nine 8-node quadrilateral elements are employed to model the solution domain (see Fig.6). The average relative error of potential u (Arerr(u)) at all boundary nodes and elementary central points is presented in Fig.7 for investigating the effect of the location of source points generated by means of Eq.(9). It can be seen from Fig.7 that an acceptable numerical accuracy can be achieved when the value of γ falls within the interval [1.5, 3.5] and the number of source points is equal to 8, 12 or 16, while the worst result is observed when $n_s = 4$ (see Fig.7). On the other hand, it can also be seen that the numerical accuracy of the results become worse if γ decreases from 1.5. This can be explained as follows. A small value of γ may cause singularity of the fundamental solution due to the close distance between the source point and field

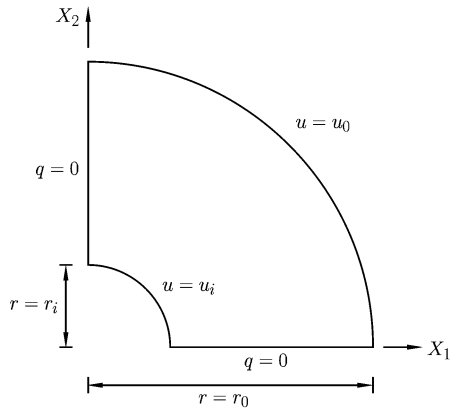

Fig. 5. Schematic diagram of a quarter of a thick cylinder and related boundary conditions.

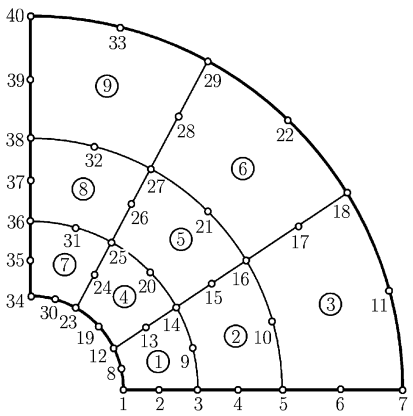

Fig. 6. 8-node quadrilateral element division for the quarter domain.

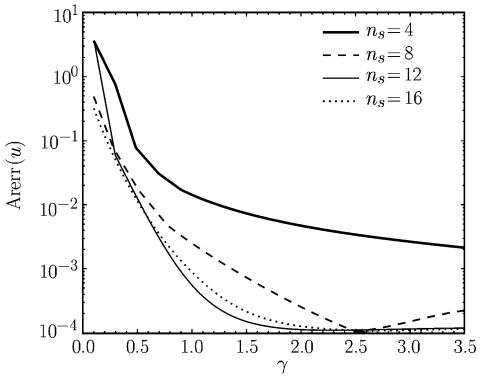

Fig. 7. Effect of various dimensionless parameter γ on numerical accuracy.

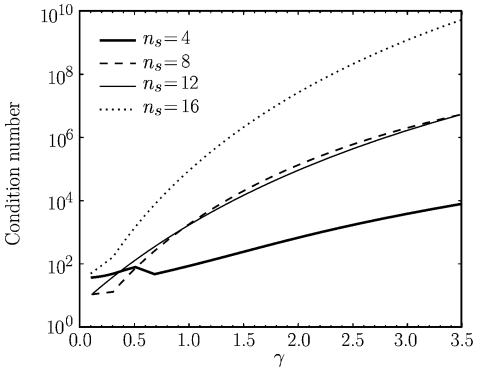

Fig. 8. Effect of various dimensionless parameter γ on the condition number of matrix $\boldsymbol{H}$.

point. Conversely, from the point of view of numerical computation, round-off error in floating point algorithms may cause another problem when the source points are far from the element boundary, that is γ has larger value, in this case, a larger condition number of the system matrix, for example the condition number of matrix $\boldsymbol{H}$ in Fig.8, may be produced. Furthermore, from Fig.8 we also observe that a larger n_s, especially $n_s = 16$, leads to a larger condition number of the matrix $\boldsymbol{H}$, and the main reason is that a larger n_s unavoidably produces the larger size of the matrix $\boldsymbol{H}$, which is not beneficial to its inverse algorithm. Therefore the optimal number of points is $n_s = 12$ and $\gamma = 2.5$, which will be used in the following computation as a general choice, unless there is a special statement. In Table 1, the distribution of numerical results along the radial direction is compared with the analytical solutions and HT-FEM. It is found from Table 1 that the results from the proposed HFS-FEM are closer to the exact solutions than those from HT-FEM.

Table 1. **Comparison of HT-FEM, HFS-FEM and analytical solutions**

Radius r	5.000	6.667	8.333	10.667	13.000	16.500	20.000
HT-FEM	10.0000	7.9255	6.3101	4.5356	3.1010	1.3889	0.0000
HFS-FEM	10.0000	7.9242	6.3156	4.5332	3.1070	1.3864	0.0000
Exact	10.0000	7.9245	6.3155	4.5342	3.1074	1.3877	0.0000

Example 2. Heat conduction in an L-shaped panel with a circular hole

In the second example, a complicated L-shaped panel with a circular hole is taken into consideration (see Fig.9) with $k = 1$. In this test, all outside boundaries are prescribed with the essential boundary

condition $u = 0$, while on the remaining inner circular boundary, $q = 10$ is presented for analysis. In the computation, the entire domain is modeled with 208 8-node quadrilateral elements and the distribution of the potential field u is plotted in Fig.10, from which we can see clearly that the results of the proposed method have a good agreement with ones of ABAQUS obtained with the same mesh division, so the proposed method can be viewed as an alternative to the conventional FEM. Additionally, although large amount of regular elements are unavoidably used in the domain division, from result comparison shown in Fig.10 we can conclude that the proposed HFS-FEM is insensitive to the mesh distortion.

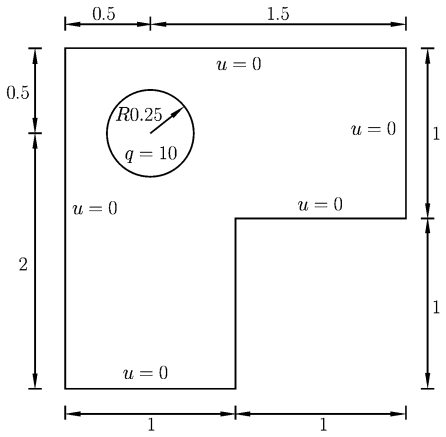

Fig. 9. The L-shaped panel with a circular hole.

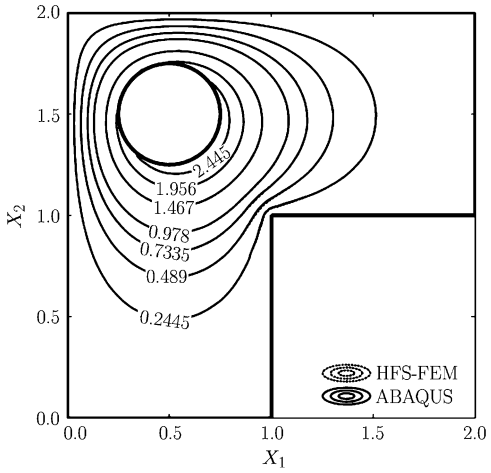

Fig. 10. Distribution of u in the L-shaped panel.

Example 3. Heat conduction in a functionally graded plate Finally, a heat conduction case in a square functionally-graded plate with boundary conditions shown in Fig.11 is studied. Assume that the plate is graded along the X_2-direction and the thermal conductivity $k = k_0 \mathrm{e}^{\beta X_2}$. β is a real parameter and k_0 a constant. In order to utilize the proposed HFS-FEM conveniently, we can introduce a stepwise constant approximation to the thermal conductivity, as shown in Fig.12. In the computation, $k_0 = 17$ W/m/°C, $\beta = 0, 20, 50\,\mathrm{m}^{-1}$, the side-length of the plate is $a = 0.04$ m. Totally 4×8 elements are used to discretize the domain and numerical results are compared to the following analytical solution with various graded parameter β in Fig.13, from which we cam see that the proposed method has good accuracy.

$$u = \frac{\mathrm{e}^{-\beta X_2} - 1}{\mathrm{e}^{-\beta a} - 1} \quad \left(\lim_{\beta \to 0} u = \frac{X_2}{a} \right) \tag{39}$$

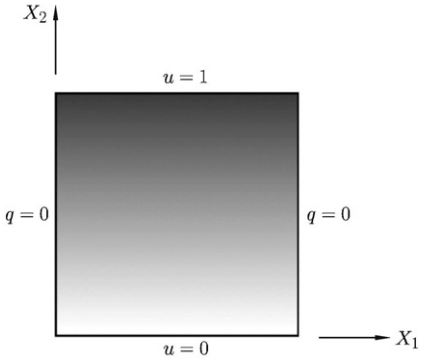

Fig. 11. Square functionally graded plate.

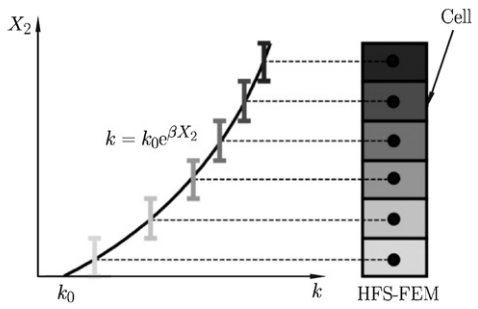

Fig. 12. Stepwise constant approximation model to the thermal conductivity.

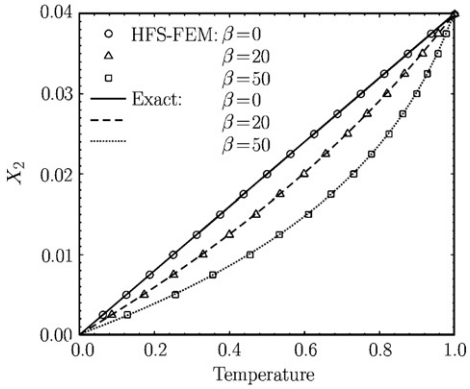

Fig. 13. Temperature distribution along the graded direction with various graded parameter β.

V. CONCLUSIONS

A new type of fundamental solution-based FEM formulation has been developed for analyzing two-dimensional heat conduction problems. In the model, a linear combination of the fundamental solution at points outside the element domain is used to approximate the field variable within an element domain, and a frame field defined on the elementary boundary is introduced to guarantee the inter-element continuity. To adapt the new trial function- fundamental solution, a modified variational functional is constructed for establishing the corresponding stiffness matrix equation. Numerical results show that the proposed method is insensitive to mesh distortion and has good accuracy. Typically, the proposed HFS-FEM has the following features:

• Compared to conventional FEM, the formulation calls for integration along the element boundaries only, which simplifies the calculation of the stiffness matrix and is easy to generate arbitrary shaped elements.

• The proposed model is insensitive to the mesh distortion and can provide good numerical accuracy.

• In contrast to the T-complete function used in HT-FEM, the fundamental solution in HFS-FEM is easy to derive, and further, the determination of source points is easier to operate than selecting appropriate terms from T-complete series in HT-FEM.

• HFS-FEM can define the fundamental solution at element level and thus can be flexibly used to analyze problems with different material properties. In contrast, BEM usually uses the fundamental solutions defined in the full domain which is not convenient for such problems with different materials. Moreover, the nonsingular boundary integrals are used in the HFS-FEM, instead of singular or hyper-singular ones in the formulation of the conventional BEM.

Although the proposed formulation and the numerical examples have been confined to heat conduction problems, extensions to complex engineering problems are possible. For example, the extension to two-dimensional elastic problems and thin plate bending problems is under way.

References

[1] Martin,H.C. and Carey,G.F., Introduction to Finite Element Analysis: Theory and Applications. New York: McGraw-Hill Book Company, 1973.

[2] Argyris,J.H., Dunne,P.C., Angelopoulos,T. and Bichat,B., Large natural strains and some special difficulties due to non-linearity and incompressibility in finite elements. *Computer Methods in Applied Mechanics and Engineering*, 1974, 4: 219-278.

[3] Tenek,L. and Argyris,J.H., Computational aspects of the natural-mode finite element method. *Communications in Numerical Methods in Engineering*, 1997, 13: 705-713.

[4] Qin,Q.H., Hybrid-trefftz finite-element method for reissner plates on an elastic-foundation. *Computer Methods in Applied Mechanics and Engineering*, 1995, 122: 379-392.

[5] Qin,Q.H., The Trefftz Finite and Boundary Element Method. Southampton: WIT Press, 2000.

[6] Jirousek,J., and Qin,Q.H., Application of hybrid-Trefftz element approach to transient heat conduction analysis. *Computers & Structures*, 1996, 58: 195-201.

[7] Qin,Q.H., Nonlinear analysis of Reissner plates on an elastic foundation by the BEM. *International Journal of Solids and Structures*, 1993, 30: 3101-3111.

[8] Kupradze,V.D. and Aleksidze,M.A., The method of functional equations for the approximate solution of certain boundary value problems. USSR *Computational Mathematics and Mathematical Physics,* 1964, 4: 82-126.

[9] Wang,H., Qin,Q.H. and Kang,Y.L., A meshless model for transient heat conduction in functionally graded materials. *Computational Mechanics*, 2006, 38: 51-60.

[10] Wang,H. and Qin,Q.H., Some problems with the method of fundamental solution using radial basis functions. *Acta Mechanica Solida Sinica*, 2007, 1: 21-29.

[11] Simpson,H.C. and Spector,S.J., On the positive of the second variation of finite elasticity. *Archive for Rational Mechanics and Analysis*, 1987, 98: 1-30.